The University of Southern Mississippi
The Aquila Digital Community

Honors Theses | Honors College

Spring 5-2018

Biocompatible, Responsive Polysoaps via RAFT Copolymerization for the Delivery of Model Cancer Therapeutics

Mason Dearborn
University of Southern Mississippi

Follow this and additional works at: https://aquila.usm.edu/honors_theses

 Part of the Polymer Chemistry Commons, and the Polymer Science Commons

Recommended Citation

Dearborn, Mason, "Biocompatible, Responsive Polysoaps via RAFT Copolymerization for the Delivery of Model Cancer Therapeutics" (2018). *Honors Theses*. 562.
https://aquila.usm.edu/honors_theses/562

This Honors College Thesis is brought to you for free and open access by the Honors College at The Aquila Digital Community. It has been accepted for inclusion in Honors Theses by an authorized administrator of The Aquila Digital Community. For more information, please contact Joshua.Cromwell@usm.edu.

The University of Southern Mississippi

Biocompatible, Responsive Polysoaps via RAFT Copolymerization for the Delivery of Model Cancer Therapeutics

by

Mason A. Dearborn

A Thesis
Submitted to the Honors College of
The University of Southern Mississippi
in Partial Fulfillment
of the Requirements for the Degree of
Bachelor of Science
in the School of Polymer Science and Engineering

May 2018

Approved by:

_____

Charles L. McCormick, Ph.D., Thesis Adviser

Professor of Polymer Science

_____

Jeffrey Wiggins, Ph.D., Director

School of Polymer Science and Engineering

_____

Ellen Weinauer, Ph.D, Dean

Honors College

Abstract

Many chemotherapeutic drugs are small, hydrophobic molecules that require water-soluble, biocompatible nanocarriers for enhanced vascular circulation. Existing polymeric carriers either conjugate the drug along a copolymer backbone or sequester drugs within a protected interior domain to be delivered to specific sites in the body. Such therapeutic systems must overcome a myriad of hurdles, beginning with complex, multi-step syntheses, followed by other inherent barriers that limit the efficiency of drug delivery at the targeted site. This work aims to circumvent a number of these issues using biocompatible, stimuli-responsive polysoaps that are capable of unimeric micelle formation, hydrophobic drug delivery, and triggered release, regardless of dilution effects. These copolymers are prepared via RAFT copolymerization of N-(2-hydroxypropyl) methacrylamide (HPMA) and dodecylpropyldisulfide methacrylamide (DPDMA). The facile synthesis of these polysoaps and their ability to function at high dilution are promising indicators of their utility in future applications.

Keywords: Drug delivery, Polysoaps, Stimuli-responsive, RAFT copolymerization

Dedication

I would like to dedicate this Honors Thesis to my loving parents,

Derek and Jackie Dearborn.

Acknowledgements

The author expresses his sincerest thanks to Phillip Pickett for his consistent mentorship and dedication across three years of research. The author would also like to thank Dr. Keith Parsons, Kaden Stevens, and Dr. Brooks Abel whose contributions to this research are greatly appreciated as well. Finally, without Dr. Charles McCormick, this incredible opportunity would not have been possible, and this research would not have been conducted with such high standards.

Table of Contents

List of Figures

List of Schemes

List of Tables

List of Abbreviations

AIBN	4,4-azobis(isobutyronitrile)
CEP	4-cyano-4-(ethylsulfanylthiocarbonyl)sulfanylpentanoic acid
CMC	critical micelle concentration
CTA	chain transfer agent
DLS	dynamic light scattering
DMF	N,N-dimethylformamide
DPDMA	(dodecylproplydisulfide)methacrylamide
EPR	enhanced permeation and retention
FTIR	Fourier transform infrared
GPC	gel permeation chromatography
HPMA	N-(2-hydroxypropyl)methacrylamide
NMR	nuclear magnetic resonance
RAFT	reversible addition-fragmentation chain transfer
SEC-MALS	size exclusion chromatography - multiple-angle light scattering
siRNA	small interfering RNA

Chapter I

Introduction and Statement of Problem

Cancer therapy state of the art

Cancer treatments today largely rely upon methods that are unable to target only cancer cells, thus limiting the extent of treatment one can receive. Therapeutic methods designed with the capability to discriminate solely against cancer are thus urgently desired. As a result of severely negative side effects and the advancement of targeted drug delivery technologies, polymeric therapeutics have rapidly become a main focus of research.[1,2] High toxicity and short half-lives of chemotherapeutic drugs have been remedied utilizing various nanoparticle-based delivery systems that encapsulate these drugs, increasing solubility and decreasing cytotoxicity to normal healthy tissues.[3,4] Due to drug-resistance development capabilities of cancer cells, therapeutic oligonucleotides, such as small interfering RNAs (siRNAs), have been explored for disrupting gene expression at the transcriptional or translational level. These otherwise promising treatments are limited by short half-lives in blood due to vulnerability to degradation by ribonucleases, and poor cellular uptake[5,6,7] Encapsulation of these oligonucleotides via polymeric nanoparticles has achieved impressive results.[8,9] Tailoring of these polymeric drug delivery systems offers opportunities for passive and active targeting of cancer cells, increasing cancer cells specificity.[10] Particularly useful are folate nanoconjugates for active targeting of the folate receptor that is overexpressed on the surface of many types of tumors, triggering receptor-mediated endocytosis of the polymer-drug conjugated system. Conjugation with this

targeting moiety has led to drug delivery directly to cancerous tissues.[11] Thus, polymeric targeted drug delivery systems have enormous potential for cancer therapy.[12]

Many types of small-molecule anti-cancer drugs, synthetic and natural compounds (plant extracts), have been extensively studied as polymer conjugates. These systems rely upon grafting of the drugs by covalent linkages that must be broken for release. Such an approach requires drug-specific polymer design and difficult synthetic challenges.[13] The investigation proposed herein focuses on facile synthetic design that requires neither grafting nor tailoring to a specific drug, since a wide variety of therapeutic molecules can be delivered from a stimuli-responsive hydrophobic domain.

Polymers in drug delivery

The central goal of a drug delivery system is to release therapeutics at a desired site within the body while maintaining an effective concentration for a desired duration. Polymer-drug and polymer-protein conjugates, polymer micelles, and polyplexes are among potential systems, allowing increased accumulation due to increased lifetime in the body, protection from breakdown by enzymes, reduction in immunogenicity, enhanced solubility, and the potential for targeting of specific anatomical sites.**Error! Bookmark not defined.**[1] A large percentage of polymer conjugate applications are for anti-cancer therapies, for which 70-fold increases in the concentrations of therapeutics have been realized in tumors via the enhanced permeation and retention (EPR) effect.[1] In addition, augmenting polymer drug delivery systems with triggered release technologies makes it possible to reach cancer cells deep within tumors.[14]

Polysoaps

Polymeric amphiphiles that have the properties of surfactants and self-assemble into ordered structures are termed polymeric micelles. Much larger in size than small-molecule surfactants, micellar polymers have widely varying architectures. These include block copolymers (macrosurfactants), stars, graft copolymers, dendrimers, segmented block copolymers, and polysoaps. In seminal research, Strauss coined the term "polysoaps" to describe statistical amphiphilic copolymers consisting of a hydrophilic backbone accompanied by hydrophobic groups that possessed surfactant-like characteristics.[15] Polysoaps are different from other surfactants in that they do not have a critical micelle concentration, since micelles are formed through intramolecular associations. In solution, without the concentration limitations of small molecule surfactants and block copolymers, polysoaps self-assemble via the hydrophobic effect[16] into unimeric or multimeric micelles of widely varying structure.[17] Polysoap applications center around exploiting the increased capacity for solubilizing hydrophobic molecules, forming intramolecular micelles capable of sequestering hydrophobes into a hydrophobic core domain even at high dilution.[18] Numerous variations in structure and charge have been studied and employed for a variety of uses, primarily for viscosity modification. Polysoap applications in drug delivery to date have been limited to polymeric micelles formed from copolymers requiring grafting;[19] however, these syntheses are multi-step, diminishing their practicality. An unexplored route to using polysoaps for drug delivery is to produce stimuli-responsive micelles that enable dissolution of the hydrophobic core domain and release of a payload inside the cancer cell (**Scheme 1**). Such a system would provide versatility in the type of hydrophobes sequestered and delivered.

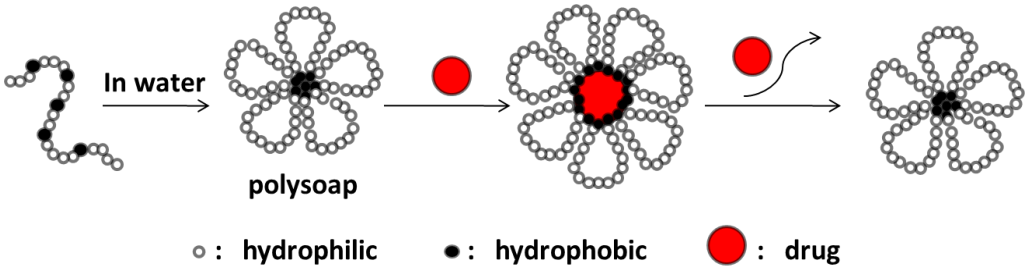

Scheme 1: Unimeric micelle or polysoap capable of drug sequestration and release in water.

Stimuli-responsiveness

As has been presented previously, drug delivery via polymeric systems offers several advantages, primarily in their capacity for controlled release of therapeutic agents.[20] Through various mechanisms, stimuli-responsiveness allows for an external stimulus to trigger various changes in the structure and properties of the delivery vehicle. These "smart polymers" can respond to many types of chemical, physical, and mechanical stimulation, with changes in temperature, ionic strength, and pH being the most commonly employed.[21] Particularly useful in cancer therapies is the incorporation of a reduction-triggered release of a drug upon delivery to the reductive microenvironment of cancer cells, inhibiting the release of the sequestered drug prior to arrival at the desired site.

RAFT polymerization

Reversible addition-fragmentation chain transfer (RAFT) polymerization, shown in **Scheme 2**, is a degenerative chain transfer polymerization technique that is both versatile and precisely controllable. It is tolerant of multiple functional groups and allows for narrow molecular weight distributions and controlled molecular weights. Polymerizations via RAFT can be conducted in aqueous solution, allowing for both reduced toxicity and safety.

In addition, the aqueous products are soluble and can be readily eliminated from the human body. A statistical RAFT copolymerization technique is quite desirable since it requires only a single synthetic step.[22] The application of this facile technique to the synthesis of polysoap drug delivery systems has potential to unlock new levels of practicality for simple and versatile drug delivery systems.

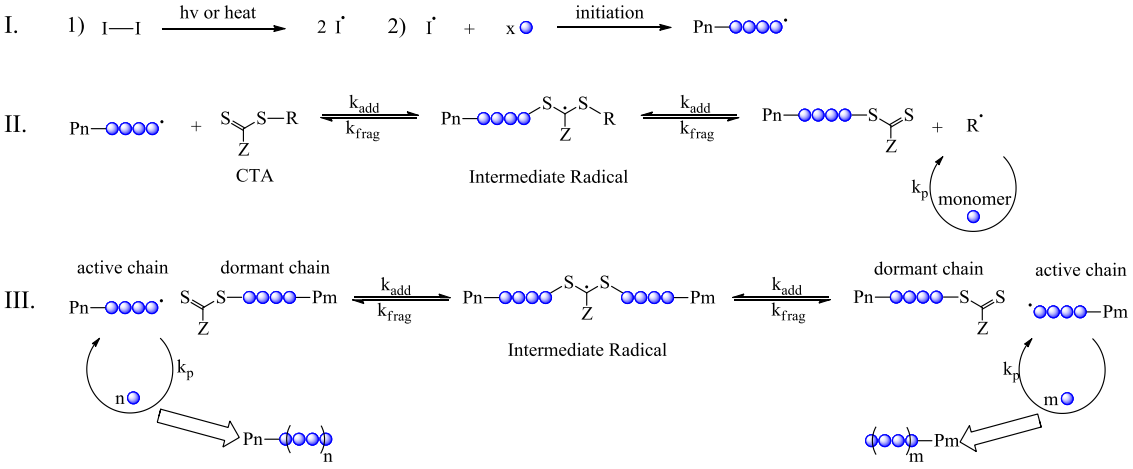

Scheme 2. Generic RAFT polymerization scheme: I) initiation; II) initialization period; III) addition/fragmentation and propagation.

Chapter II

Objectives of Research

The overall goal of this research project was to develop a bio-compatible polysoap that is capable of triggered drug release *in vivo*. To do this, we have designed a polysoap scaffold that allows for the dissociation of the hydrophobic domain in the presence of the reducing environment of the cytoplasm, allowing for triggered intracellular drug release. This design laid the groundwork for future systems with potential to take up, transport, and release hydrophobic cancer therapeutic drugs in the body regardless of micelle concentration. To realize the full potential of this design, the objectives of this research proposal were to:

1) Prepare biocompatible, responsive polysoaps via RAFT copolymerization of HPMA and DPDMA.
2) Measure micelle properties in water using DLS, UV-Vis, and fluorescence spectroscopy.
3) Determine model hydrophobe uptake and release efficiencies of the polysoaps in water.
4) Determine toxicity of polysoaps.

This research can be divided into four main sections: monomer and polymer synthesis, polysoap properties in water, hydrophobe uptake and release studies, and cell toxicity studies. The first section involved the detailed synthesis of the monomers and copolymers to achieve the polysoap of interest. Standard techniques such as nuclear magnetic resonance (NMR) and Fourier transform infrared (FTIR) spectroscopy were used

to confirm the structure of the monomers and copolymer. Molecular weight and molecular weight distribution of the copolymers were determined using size exclusion chromatography coupled to multiple-angle light scattering (SEC-MALS). The second section reports DLS, UV-Vis spectroscopy, and fluorescence spectroscopy studies, used to study micelle formation and hydrophobe uptake properties in water. The third section details the ability of the polysoap to retain and release hydrophobic molecules in water and in the presence of the reducing molecule, glutathione. The fourth section reports the toxicity of the polysoaps using an MTT cell viability assay.

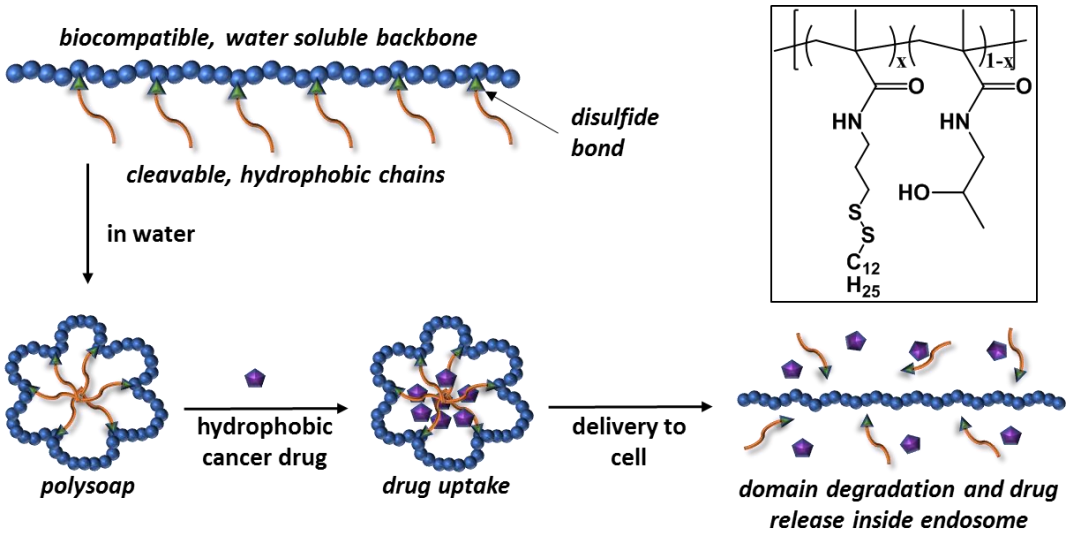

Scheme 3. The structure of the targeted polysoap is shown with its mechanism of uptake and release of hydrophobic cancer drug.

Chapter III

Materials and Methods

Materials

The monomer precursors D,L-1-amino-2-propanol (TCI, 98%), sodium methanesulfinate (AK Scientific, 92%), sulfur (Sigma Aldrich, 100 mesh), bromo propylamine hydrobromide (AK Scientific, 98%), and dodecanethiol (Sigma Aldrich, 98%) were used as received. Methacryloyl chloride (Aldrich, 97%) was distilled under vacuum and stored under N_2 at −10 °C prior to use. The RAFT agent precursors ethanethiol (Sigma Aldrich, 98%), carbon disulfide (Sigma Aldrich, 99.9%), and 4,4′-azobis(4-cyanopentanoic acid) (V-501) were used as received. The solvents diethyl ether (Fisher Scientific, Spectranalyzed), pentane (Fisher Scientific, HPLC grade), acetone (Fisher Scientific, Optima grade), anhydrous methanol (Sigma Aldrich), and 200 proof ethanol (Decan Laboratories, anhydrous) were used as received. The initiator (96%) 2,2′-azobis(2-methylpropionitrile) (AIBN) was purchased from Sigma Aldrich and recrystallized from methanol prior to use. The internal standard, trioxane, was purchased from Sigma-Aldrich and used as received. The detailed synthesis of the RAFT chain transfer agent 4-cyano-4-(ethylsulfanylthiocarbonylsulfanyl)pentanoic acid (CEP) and monomers N-(2-hydroxypropyl)methacrylamide (HPMA) and (dodecylpropyldisulfide)methacrylamide (DPDMA) are described below.

Synthesis of 4-cyano-4-(ethylsulfanylthiocarbonyl)sulfanylpentanoic acid (CEP)

Using a procedure as previously reported,[23] a suspension of sodium hydride (95%) (2.11 g, 83.5 mmol) in anhydrous diethyl ether (150 mL) was cooled to 0 °C using an ice bath, upon which ethanethiol (5.73 g, 92.3 mmol) was added over 15 min accompanied by a vigorous evolution of hydrogen gas. The reaction was stirred for an additional 15 min at 0 °C followed by dropwise addition of carbon disulfide (7.03 g, 92.3 mmol) over 5 min and the reaction stirred for 60 min at room temperature. The reaction solution was then diluted with pentane (100 mL) and the resulting yellow precipitate isolated by vacuum filtration before drying under vacuum to yield sodium ethyl trithiocarbonate (12.07 g, 90%) as a hygroscopic yellow solid. To a suspension of sodium ethyl trithiocarbonate (9.89 g, 61.7 mmol) in diethyl ether (200 mL) at room temperature was added solid I_2 (8.63 g, 34.0 mmol) over 5 min. The reaction was stirred for 60 min at room temperature and the precipitated sodium iodide salts were removed by vacuum filtration and washed with 50 mL of diethyl ether. The filtrate was transferred to a separatory funnel and washed with 5% sodium dithionite (1 x 150 mL), deionized water (1 x 150 mL), and brine (1 x 150 mL) before drying over anhydrous magnesium sulfate. The solvent was removed via rotary evaporation followed by drying in vacuo to yield bis(ethyl) trithiocarbonate (96%) as a yellow solid. A solution of bis(ethyl) trithiocarbonate (5.00 g, 18.2 mmol) and V-501 (7.66 g, 27.3 mmol) in ethyl acetate (250 mL) was prepared in a 500-mL 3-necked flask equipped with stir bar and condenser. The solution was purged with N_2 for 40 min prior to heating at reflux for 18 hrs, upon which the reaction was quenched via exposure to air and cooled to room temperature. The solvent was removed via rotary evaporation and the crude RAFT agent purified via column chromatography on silicon dioxide (60:35:5 hexanes:ethyl

acetate:acetic acid). To remove the acetic acid, the column fractions containing CEP were combined and transferred to a separatory funnel and washed with 0.05 N hydrochloric acid (2 x 150 mL) and brine (1 x 150 mL) and dried over magnesium sulfate, and the solvent removed via rotary evaporation followed by drying under vacuum to yield CEP as a yellow solid. Yield: 7.10 g (74%); mp: 58-60 °C; ^{1}H NMR (300 MHz, $CDCl_3$): δ 3.38 (q, 2H), 2.70 (t, 2H), 2.55 (m, 2H), 1.85 (s, 3H), 1.40 (t, 3H) (**Figure A1**).

Synthesis of N-(2-hydroxypropyl)methacrylamide (HPMA)

Using a procedure as previously reported,[24] to a 2-L round bottom flask was added D,L-1-amino-2-propanol (102.307 g) dissolved in 1 L of acetonitrile. A stir bar was added, and the round bottom flask was sealed with a septum and placed into an ice bath. To the reaction mixture was added methacryloyl chloride (67.80 g) dropwise over 3 hrs. The round bottom flask was then removed from the ice bath and allowed to reach room temperature, and then the contents were stirred for an additional 2 hrs. Solvent was removed via rotary evaporation at 30 ^{o}C. After 2/3 of the solvent had been removed, a white crystalline salt formed. The salt was isolated via vacuum filtration and purified by recrystallization from minimal acetone at room temperature. The resulting product was white crystals. mp: 65-67 °C; ^{1}H NMR (300 MHz, D_2O): δ 6.60 (b, 1H), 5.70 (s, 1H), 5.30 (s, 1H), 3.90 (b, 1H), 3.70 (d, 1H), 3.10-3.60 (m, 2H), 1.9 (s, 3H), 1.2 (d, 3H) (**Figure A2**).

Synthesis of (dodecylproplydisulfide) methacrylamide (DPDMA)

A mixture of sodium methanesulfinate (10 g, 98 mmol) and sulfur (3.14 g, 98 mmol) in dry methanol (1.2 L) was heated to reflux using a heating manifold (set voltage

to 50 V) and a condenser (with drying tube inserted into a rubber septum). After 18 hrs, the sulfur had dissolved, and the reaction was stopped. The solvent was removed by rotary evaporation, leaving behind an off-white residue. To the residue was added 500 mL of 200 proof ethanol to dissolve the desired product. After stirring for 1 hrs, not all the solids had dissolved, and the solution was filtered via vacuum filtration. The filtrate was then concentrated by rotary evaporation and the product was dried under high vacuum for 4 hrs, resulting in a white powder, sodium methanethiosulfonate. To a round bottom flask containing water (150 mL), bromo propylamine hydrobromide (5.04 g, 23.0 mmol) and sodium methanethiosulfonate (6.01 g, 44.8 mmol) were added. The mixture was stirred at 70 °C for 18 hrs. The reaction was then removed from the heat and the solvent was removed via rotary evaporation, leaving an off-white powder. The crude powder was then triturated using ethanol. The solution became light yellow and the powder became white as impurities dissolved. The product was collected via vacuum filtration and washed with ethanol, followed by drying overnight under high vacuum. The pure product was a white powder, aminopropyl sodium methanethiosulfonate. Aminopropyl sodium methanethiosulfonate (11.25 g, 54.6 mmol) was dissolved in dry methanol (200 mL), and dodecanethiol (80 mL, 332 mmol) was added and the solution was stirred for 18 hrs at room temperature. The contents of the reaction were then transferred to a separatory funnel. The excess dodecane thiol was the bottom layer and methanol the top layer. The dodecane thiol was removed from the methanol and then hexanes were added to the separatory funnel to wash the methanol layer. The product remained in the bottom methanol layer. The methanol layer was removed and concentrated using rotary evaporation, leaving a white powder. The product was washed with hexanes and collected via vacuum filtration and

dried via high vacuum. The product was further purified via column chromatography on silica gel using chloroform with 3% triethylamine as the eluent. After the product was isolated, it was a white powder, aminopropyl dodecyl disulfide. Aminopropyl dodecyl disulfide (14.0 g, 43.0 mmol) was added to a round bottom flask. To the flask were then added 300 mL of acetone and triethylamine (15.0 mL). The flask was charged with a stir bar, sealed with a rubber septum, and placed in an ice bath. Methacroylchloride (7.0 mL, 71.6 mmol) was then added dropwise while stirring in the ice bath. The vessel was removed from the ice bath and allowed to reach room temperature, and the reagents stirred for an additional 18 hrs. A white precipitate had formed after adding the methacroylchloide, and it was removed via vacuum filtration. The supernatant was then collected and removed via rotary evaporation, leaving a brownish orange oil. The crude product was then purified via column chromatography using chloroform as the eluent. The pure product was isolated and dried under high vacuum, resulting in a white powder, (dodecylpropyldisulfide) methacrylamide. Yield: 4.0 g (25%); mp: 41-43 °C; ^{1}H NMR (300 MHz, $CDCl_3$): δ 5.98 (s, 1H), 5.70 (s, 1H), 5.30 (s, 1H), 3.45 (q, 2H), 2.70 (q, 4H), 1.98 (b, 5H), 1.65, (m, 2H), 1.25 (b, 18H), 0.80 (t, 3H) (**Figures A3-A6**).

Statistical copolymerization of HPMA and DPDMA via RAFT

The general procedure is as follows: the HPMA, DPDMA, CEP, and AIBN with desired feed ratios were added to a 25-mL polymerization flask equipped with a magnetic stir bar. For example, HPMA (2.83 g, 19.9 mmol), DPDMA (0.377 g, 1.05 mmol), CEP (6.50 mg, 24.7 μmol), methanol (20 mL), and AIBN (0.811 mg, 4.94 μmol) were added with the molar ratios of HPMA:DPDMA:CEP:AIBN = 950:50:1:0.2. Trioxane (250 mg)

was added as an internal standard. The flask was then sealed and purged with ultra-high purity N_2. After purging with N_2 for 60 min, an initial aliquot of 200 μL was taken prior to commencing the polymerization at 70 °C in an oil bath while stirring. After the desired polymerization time of 48 hrs, an aliquot was taken and analyzed by ^{1}H NMR (MeOH-d4) to determine monomer conversion by comparing the relative integral areas of the signal from the trioxane protons to those of the monomer vinyl protons. An SEC-MALS instrument (eluent of 0.2 M $LiClO_4$ in methanol) was used to monitor the molecular weight and molecular weight distribution (M_w/M_n) of each polymerization. The polymer was purified via precipitation from acetone and isolated via centrifugation. The polymer pellet was then washed with acetone five times, followed by drying overnight under vacuum to yield a white powder. The final product was analyzed by ^{1}H-NMR in MeOH-d4 (**Figures A7** and **A8**).

Preparation of polysoap solutions

Polysoaps were solubilized in deionized water, followed by sonication, vortexing, and shaking for 48 hrs. Solutions were prepared via serial dilutions, using an automatic micropipette and 25-mL volumetric flasks for precision. This yielded solutions with concentrations of 0.1, 0.5, 1.0, 3.75, and 5.0 mg/mL in deionized water.

Pyrene uptake into the core domains of the polysoaps

To study the uptake characteristics of the polysoaps, the following procedure was used for a single trial: to a single 1.5-mL centrifuge tube was added 10 μL of 50 mg/mL pyrene solution in acetone. The acetone was evaporated, leaving the pyrene behind. Into

the centrifuge tube was then added the desired polysoap solution in water (1.5 mL). The contents were vortexed and allowed to shake for 24 hrs for the solution to equilibrate. Then the solution was centrifuged, and 1 mL of the polysoap/pyrene solution was transferred to another centrifuge tube prior to measurement of pyrene absorbance and I_3/I_1 ratios via UV-Vis spectroscopy and fluorescence spectroscopy, respectively.

Hydrocarbon retention and release experiments

Hydrocarbon retention in water was performed using the following procedure: into a 1.5-mL centrifuge tube was added 1 mL of 5 mg/mL polysoap solution. The solution was prepared using 0.1 mM 9-anthracenemethanol. The contents of the centrifuge tube were allowed to equilibrate over 24 hrs. Then the solution was transferred to a dialysis bag (molecular weight cutoff of 1,000 g/mol). The bag with the solution was then dialyzed against deionized water. An initial aliquot was taken for UV-Vis spectroscopy, followed by sampling and absorbance measurements at desired times. Each aliquot was returned to the dialysate after measurement. After several measurements, 50 mmol of glutathione was added to the dialysate and aliquots were taken and measured via UV-Vis spectroscopy.

The following procedure was used for the hydrocarbon release experiment: to a 50-mL centrifuge tube was added 5 mL of 5 mg/mL polysoap solution. The solution was prepared using 0.1 mM 9-anthracenemethanol. The contents of the centrifuge tube were allowed to equilibrate over 24 hrs. Ethyl acetate (5 mL) was added to the centrifuge at the start of the experiment. An initial aliquot of the ethyl acetate was taken for UV-Vis spectroscopy followed by sampling and measurement of the ethyl acetate layer at desired times. Each aliquot was returned to the centrifuge tube after measurement. After several

measurements, 50 mmol of glutathione was added to the centrifuge tube and aliquots were taken and their absorbances measured via UV-Vis spectroscopy.

Cell toxicity experiment

To determine cell toxicity of the polysoaps, a standard MTT cell assay was conducted.[25] Cervical adenocarcinoma (KB) cells (10,000 cells per mL, 100 μL) were seeded in a 96-well plate (Corning Inc.) in a phosphate-buffered saline solution. Cells were treated with 10 μL of a polymer stock solution (50, 25, 10, and 5 μg/mL). Cell proliferation was determined via a standard MTT assay (Vybrant MTT Cell Proliferation Assay Kit; Invitrogen). Cells were incubated for 24 hrs prior to adding 10 μL of the 12 mM MTT reagent to each well. The cells were incubated for an additional 4 hrs, followed by adding 100 μL of a sodium dodecyl sulfate (10%)/hydrochloric acid (0.01 M) solution to each well. The absorbance was then determined utilizing a Biotek Synergy2 MultiMode Microplate Reader. All studies were performed in triplicate.

Characterization of polysoaps

Dynamic light scattering (DLS) data were collected using incident light at 633 nm from a Research Electro Optics HeNe laser operating at 40 mW. The time-dependent scattering intensities were measured with a Brookhaven Instruments BI-200SM goniometer at 60, 75, 90, 105, and 120^{o} with an avalanche photodiode detector and TurboCorr correlator. The decay rate was collected from a quadratic fit of the autocorrelation function. The data was processed using Mathcad with the following steps: decay rate was plotted versus q^2 to generate a straight line. The slope of the line is the

diffusion coefficient. The diffusion coefficient was then used in the Stokes-Einstein equation to calculate the hydrodynamic radius of the particles. The radius was multiplied by two to produce the hydrodynamic diameter, which was reported for the DLS experimental data. An example of the DLS data processing can be found in the appendix (**Figure A9**).

Gel permeation chromatography (GPC) was performed using an assembled instrument with a Hewett Packard Series 1100 HPLC pump in-line with a Viscotek T60A Dual Detector and a Viscotek VE3580 IR detector. The GPC system was equipped with Tosoh TSKgel Super AW guard column, Super AW3000, and Super AW4000 columns in series. The eluent used for the polysoap was 0.2 M lithium perchlorate in methanol. The SEC software used to process the data was OmniSEC version 4.7.

All UV-Vis spectroscopy measurements were performed with an Agilent Technologies Carey Series UV-Vis-NIR Spectrophotometer run by Carey WinUV software. All steady-state fluorescence measurements were performed with a PTI-Horiba QuantaMaster 400 spectrofluorimeter equipped with a 75 W Xe arc lamp.

Chapter IV

Results and Discussion

Structural design of biocompatible polysoaps

To study the solution properties and feasibility for drug delivery of responsive polysoaps, we prepared two statistical copolymers via the RAFT copolymerization of HPMA and DPDMA (**Scheme 4**). The DPDMA monomer was designed to form the hydrophobic domain of the micelles. Additionally, as desired for our polysoap design, the hydrophobic dodecyl disulfide functionality has the ability to be reductively cleaved to a thiol, providing for responsive hydrophobic domain dissociation and drug release. The HPMA monomer was chosen to form the water-soluble corona of the micelles and is biocompatible and non-immunogenic. Monomer content for this study was based on previous work conducted in our group,[26] which indicated the necessity of sufficient hydrophobic content to form core domains in the micelles. However, since the coronas in our polymeric micelles are neutral, water solubility can be compromised with too high a hydrophobic content. To ensure water solubility and micelle formation, mole percentages of 5% and 10% DPDMA were targeted. The resulting copolymers had weight average molecular weights of 37.9 and 33.7 kDa and M_w/M_n values of 1.08 and 1.09, respectively (**Table 1)**. **Figure 1** shows the SEC traces of the polysoap samples. From these traces we observed that the polymerizations resulted in narrow and unimodal molecular weight distributions, characteristics that are necessary for well-defined micelles for drug delivery applications.

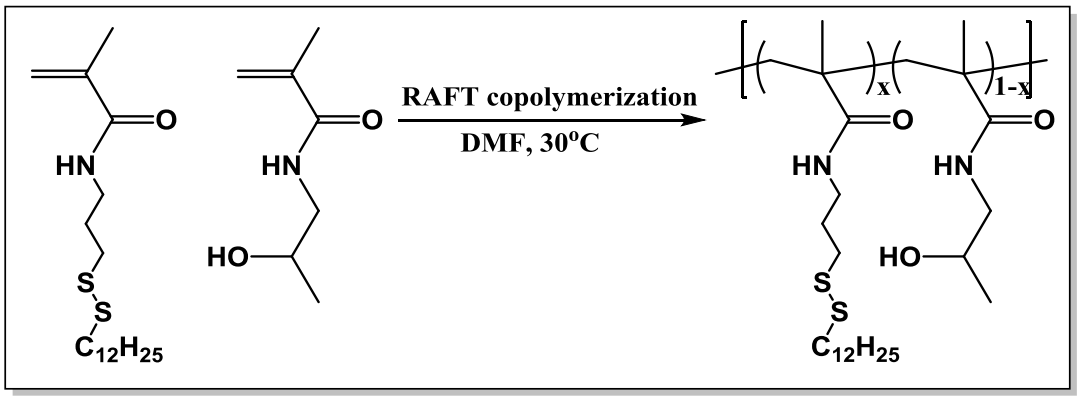

Scheme 4. Synthesis of biocompatible, responsive polysoap poly(DPDMA-stat-HPMA).

Table 1. Structural details of poly(DPDMA-stat-HPMA) series.*

Sample	Conversion[a]	DPDMA Content[a]	M_w/kDa[b]	M_w/M_n
5% DPDMA	33%	7.77%	37.9	1.08
10% DPDMA	33%	15.4%	33.8	1.06

[a]Determined by ^{1}H NMR.
[b]Determined by SEC-MALS.
*All polymerizations were conducted at 30 °C in dimethylformamide until the desired monomer conversion was achieved.

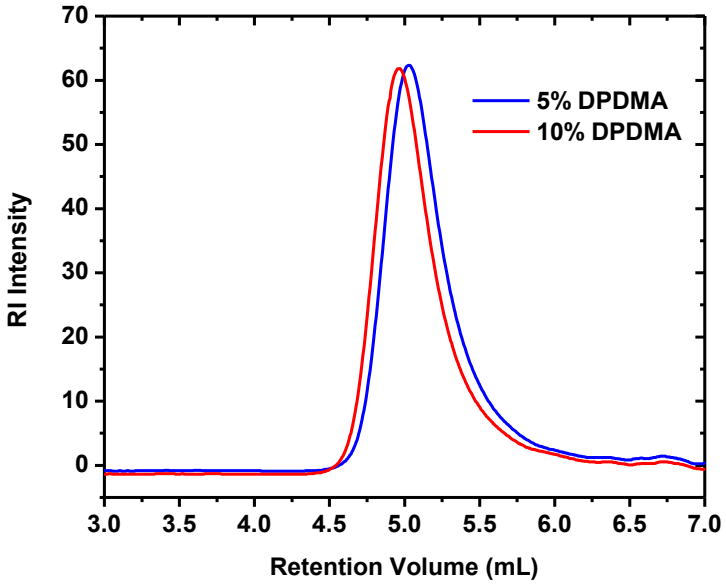

Figure 1. Size exclusion chromatography (SEC) traces of polysoaps. Eluent: 0.05 M $LiClO_4$ in MeOH. Flow rate: 0.3 mL/min.

Polysoap properties in water

It was expected that the polysoap micelles would arrange into well-defined particles of specific sizes. Dynamic light scattering (DLS) is a well-understood technique that allows for the determination of the hydrodynamic diameters of the respective polysoap micelles in water as a function of polymer concentration (**Figure 2a**). The size of the 5% DPDMA sample indicates that a unimeric micelle is possibly formed, with consistent values of approximately 11 nm across the concentration range measured. The 10% DPDMA sample, however, exhibits larger relative sizes of around 60 nm, suggesting that multimeric micelles or aggregates are formed. This can be attributed to increased hydrophobicity, and, without a charged corona to stabilize the micelle electrosterically, inter-core mixing may be prominent at higher hydrophobic contents. Notably, the hydrodynamic diameters of both samples do not increase with concentration, which reveals that the uni- and multi-meric micelles of the 5% and 10% DPDMA polysoaps, respectively, are stable at the experimentally measured concentrations and hydrophobic contents.

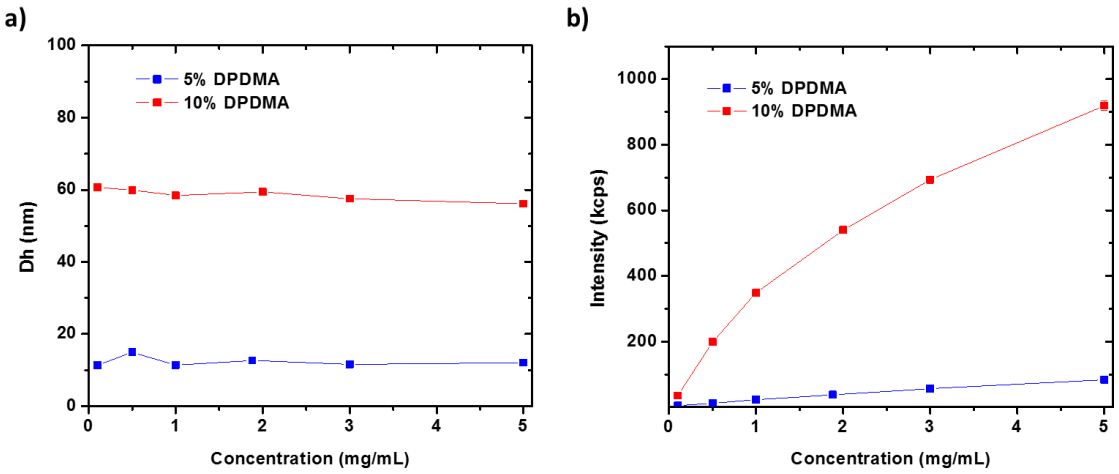

Figure 2. a) Hydrodynamic diameter dependence on polysoap concentration in water as measured by dynamic light scattering; b) Scattering intensity dependence on polysoap concentration in water as measured by static light scattering at 90°.

In **Figure 2b**, the scattering intensity of the polysoap solutions as a function of polymer concentration is shown. The sample with 10% molar hydrophobe content has consistently higher intensities and a greater slope compared to the 5% polysoap sample. Since scattering intensity scales with the size of a point scatterer, this is in agreement with larger particle sizes being observed in the DLS experiments for the 10% samples. The scattering intensity is also shown to increase relatively linearly with concentration, indicating a consistent aggregation number and size of the copolymers in solution.

Once the formation of particles was confirmed via DLS, the nature of the hydrophobic core domains was probed. This was accomplished through fluorescence spectroscopy measurements of pyrene in solution with respect to increasing concentration of polysoap. The intensity of the vibronic peaks in the fluorescent spectrum of pyrene changes with the hydrophobicity of the microenvironment of the pyrene.[27,28] Specifically, the ratio of the intensity of the third to the first vibronic peak of pyrene increases as the environment of the pyrene becomes more hydrophobic. As is shown in **Figure 3**, pyrene becomes associated with the hydrophobic core domain of the polysoap micelles. As the polysoap concentration increases, so does the I_3/I_1 ratio, indicating a more defined hydrophobic microdomain in the core of the micelles. Furthermore, it is observed that 10% DPDMA with its higher hydrophobic content elevates the ratio of the peak intensities more than does 5% DPDMA. An interesting observation is the increase in ratio with polymer concentration. This indicates that the domains are becoming more hydrophobic as polymer concentration increases. This is unexpected for unimeric micelles but is observed in both the 10% and 5% DPDMA systems, suggesting multimeric aggregates for these systems.

Regardless, micelles form even at very low concentrations of 0.1 mg/mL, indicated by particle formation and some degree of hydrophobic core definition.

Next, the capacity for hydrocarbon uptake was tested and measured using UV-Vis spectroscopy. Shown in **Figure 4**, the absorbance of pyrene increased with increasing polysoap concentration in deionized water. This demonstrates the ability of the polysoaps to take up hydrocarbon, as increased amounts of polysoap are seen to correlate linearly with increased amounts of pyrene dispersed in solution. In addition, of the two samples, the 10% DPDMA exhibited greater uptake efficiency, indicative of larger or more well-defined hydrophobic core domains with increased hydrophobe content and consistent with the elevated I_3/I_1 ratios from the fluorescence experiments. The 5% DPDMA still sequesters pyrene but to a lesser extent. Nonetheless, both samples have the capability to disperse pyrene even at lower concentrations.

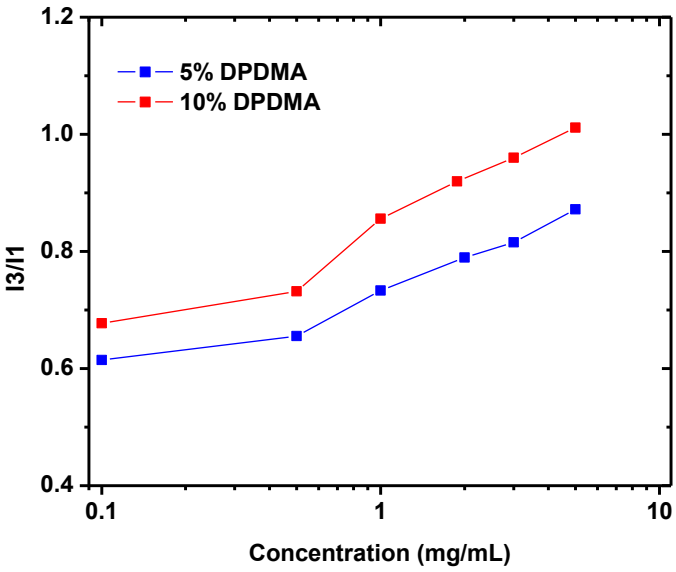

Figure 3. Probing the hydrophobic domain of the polysoaps at varying concentrations using pyrene I_3/I_1 ratios.

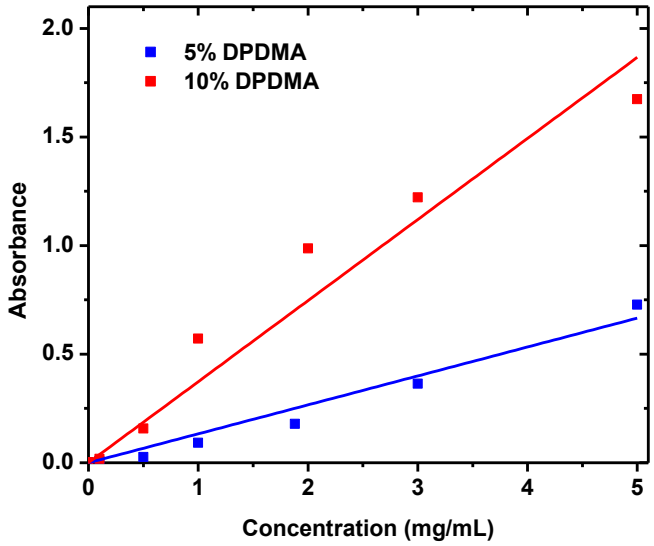

Figure 4. Pyrene sequestration as measured by UV-absorbance at 338 nm as a function of polysoap concentration.

Hydrocarbon retention and release experiments

Thus far, it has been demonstrated that polysoaps in aqueous solution form micelles with core domains capable of hydrocarbon uptake. Next, we studied the retention and triggered release of hydrocarbon, both essential for effective drug delivery. First, the polysoaps were studied relative to hydrocarbon retention and release in the presence and absence of glutathione as the reducing agent. 9-Anthracenemethanol was used as a model hydrophobe capable of partitioning into water to a small extent. This experiment relied on dialysis of the analyte through a membrane that retained the polymer. A signal in the dialysate indicates hydrocarbon release. As shown in **Figure 5**, the polysoap was sufficient at retaining the hydrocarbon in water. Additionally, glutathione was observed to be ineffective as a reducing agent in the time frame of the experiment, as its addition to solution did not significantly increase the relative absorbance of the hydrophobe in the dialysate. Had the desired release mechanism occurred, the glutathione would have reduced

the disulfide bond of the DPDMA units, changing those units to hydrophilic, and thus disrupting the hydrophobic core domain. This would have triggered the release of the sequestered hydrophobe and would have resulted in an increase in relative absorbance of the dialysate. Instead, the rate of increase of the relative absorbance seems unaffected by the addition of glutathione, suggesting insufficient domain formation or the absence of the desired disulfide bond cleavage. The desired release mechanism is obviously not operative, and the reason must be determined before charting a new strategy for the application of this technology to drug delivery.

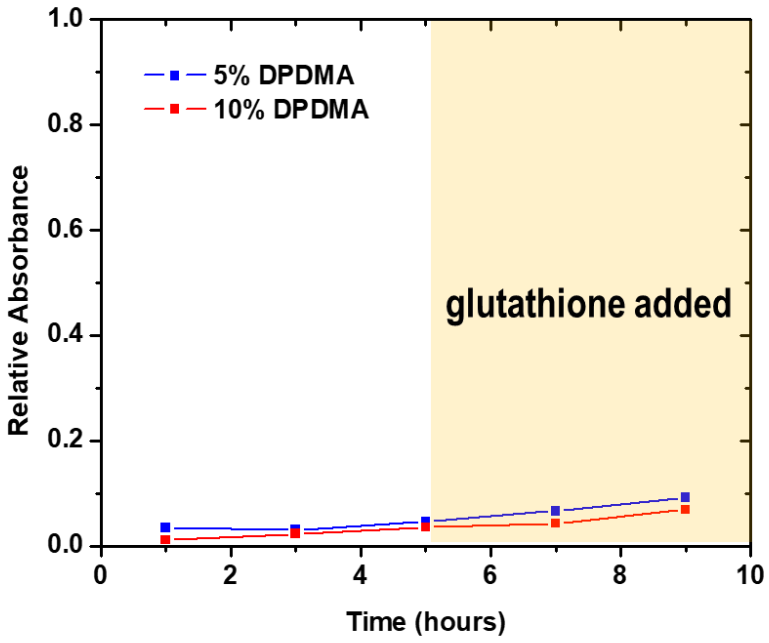

Figure 5. Absorbance of 9-anthracenemethanol in dialysate via dialysis against water. The dialysis bag contained 1 mL of polymer solution (5 mg/mL).

Retention of the hydrocarbon in the presence of a nonpolar solvent was also examined. For proper circulation of a loaded drug delivery vehicle until it has reached its target, the vehicle must not prematurely release or leak its drug payload. As partitioning of the payload to other tissue may occur inside the body, it is important to determine if this

will occur. As is shown in **Figure 6**, using ethyl acetate, an organic solvent, premature partitioning of the 9-anthracenemethanol into the organic layer occurred. This is undesired, as the loaded drug delivery vehicle needs to be able to retain its payload in similarly hydrophobic areas in the body, such as in fat tissue. Furthermore, the addition of glutathione had no significant effect on the release of hydrophobe, likely due to significant release of hydrophobe prior to glutathione addition. This illustrates that the polysoap system of this study must be altered to increase hydrophobic core domain stability and definition to avoid premature partitioning of the hydrophobe from the delivery vehicle and increase hydrophobe retention.

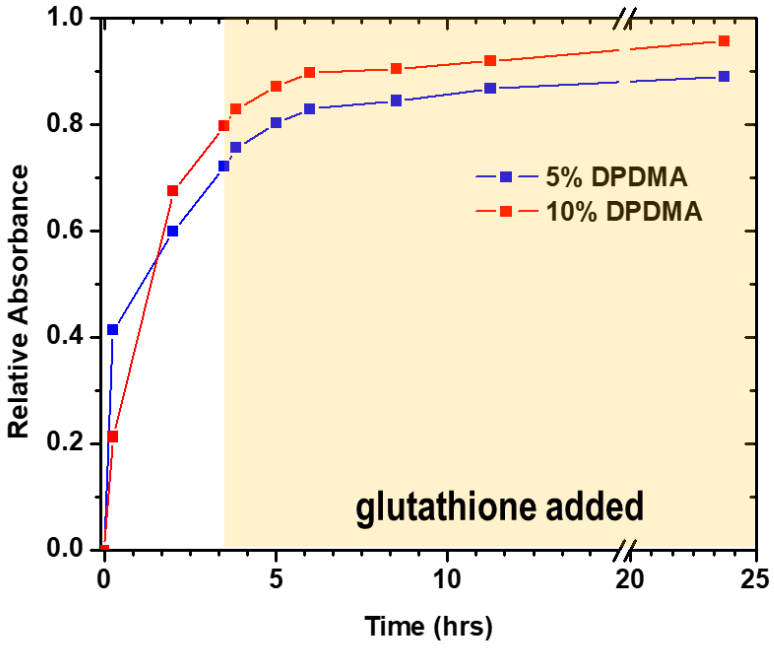

Figure 6. Absorbance of 9-anthracenemethanol in ethyl acetate (5 mL) via extraction from 5 mL of polymer solution (5 mg/mL).

Cell toxicity

Finally, the cell toxicity of the polysoaps was tested to determine biocompatibility with KB cells. As is seen in **Figure 7**, relative to the control, the toxicity of all the tested concentrations of polysoap was negligible for both polymer samples. Differences in toxicity in this test are within experimental error, which was large for the tests performed. Further experiments with larger sample sizes will be required for statistical confirmation of the overall toxicity; however, initial experiments conclude that these polysoaps may safely be used *in vitro*.

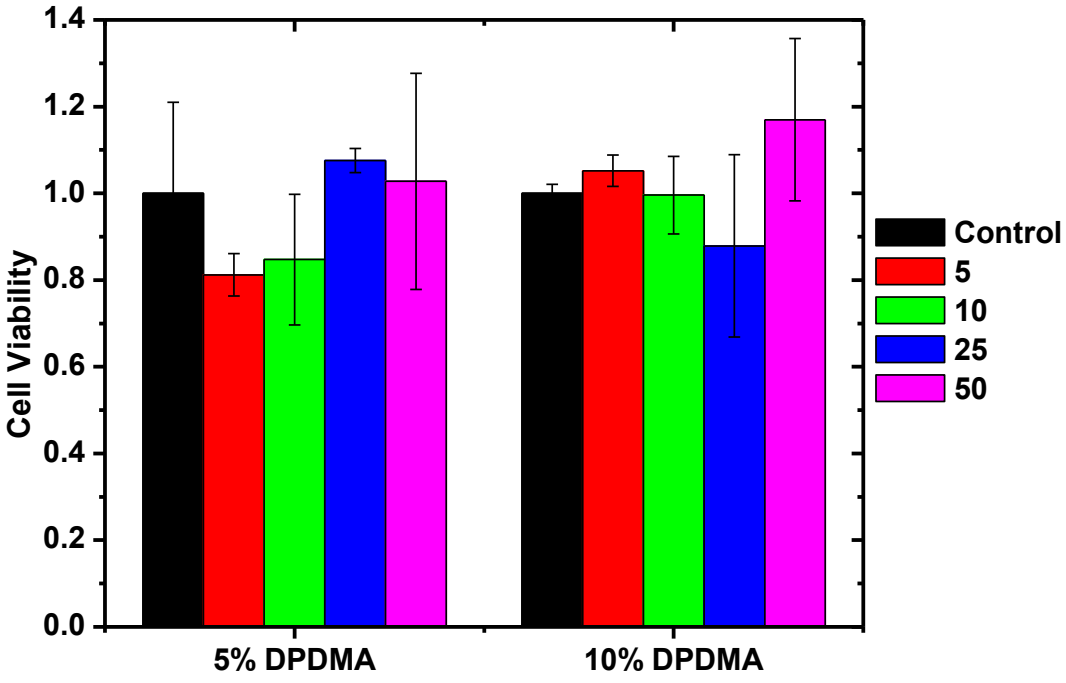

Figure 7. Cell viability determined via MTT cell assay at different concentrations of polymer sample, in µg/mL.

Chapter V

Conclusions

A series of biocompatible, responsive polysoaps was prepared via RAFT copolymerization. As determined by DLS, UV-Vis, and fluorescence spectroscopy, the polysoaps assemble into micelles that possess domains capable of sequestering hydrocarbons in water. Hydrocarbon retention experiments during dialysis against water suggest that the micelle core domains retain 9-anthracenemethanol in water, indicated by relatively small amount of hydrophobe in the dialysate. Furthermore, addition of glutathione to the dialysis solution did not result in the expected release of the hydrocarbon within the time frame of the experiment. Hydrocarbon partitioning experiments in the presence of ethyl acetate indicate that the polysoaps do not retain the hydrophobe, with nearly complete partitioning of 9-anthracenemethanol into the organic layer. Additionally, the partitioning did not require glutathione cleavage of the disulfide linkage. The polysoaps are relatively non-toxic, as determined by a minimal decrease in cell viability as compared to the control. Though the polysoap design is promising for drug delivery based on efficient hydrocarbon uptake and biocompatibility, further studies and alterations to the structural design will be necessary to optimize hydrocarbon retention and triggered release for such applications.

References

[1] Duncan R. *Nat Rev Drug Discov***. 2003**; 2 (5): 347-60.

[2] Duncan R. *Nat Rev Cancer*. **2006**; 6 (9): 688-701

[3] M. A. Phillips, M. L. Gran and N. A. Peppas, *Nano today*, **2010**, 5, 143-159.

[4] W. B. Liechty and N. A. Peppas, *European journal of pharmaceutics and biopharmaceutics : official journal of Arbeitsgemeinschaft fur Pharmazeutische Verfahrenstechnik* e.V**, 2012**, 80, 241-246.

[5] M. Creixell and N. A. Peppas, *Nano today*, **2012**, 7, 367-379.

[6] S. H. Chen and G. Zhaori, *European journal of clinical investigation*, **2011**, 41, 221-232.

[7] K. Raemdonck, T. F. Martens, K. Braeckmans, J. Demeester and S. C. De Smedt, *Advanced drug delivery reviews*, **2013,** 65, 1123-1147.

[8] T. Kato, A. Natsume, H. Toda, H. Iwamizu, T. Sugita, R. Hachisu, R. Watanabe, K. Yuki, K. Motomura, K. Bankiewicz and T. Wakabayashi, *Gene therapy*, **2010**, 17, 1363-1371.

[9] K. Nakamura, A. S. Abu Lila, M. Matsunaga, Y. Doi, T. Ishida and H. Kiwada, *Molecular therapy: the journal of the American Society of Gene Therapy*, **2011**, 19, 2040-2047.

[10] Mousa SA, Bharali DJ. Nanotechnology-based detection and targeted therapy in cancer: nano-bio paradigms and applications. *Cancers (Basel)*. **2011** Jul 15; 3(3):2888-903.

[11] Yoo HS, Park TG. Folate-receptor-targeted delivery of doxorubicin nano-aggregates stabilized by doxorubicin-PEG-folate conjugate. *J Control Release*. **2004** Nov 24; 100 (2): 247-56.

[12] Kegang Liu, Xiaohua Jiang and Patrick Hunziker. Carbohydrate-based amphiphilic nano delivery system for cancer therapy. *Nanoscale.* **2016.**

[13] M. E. Wall, M. C. Wani, C. E. Cook, K. H. Palmer, A. T. McPhail and G. A. Sim, *Journal of the American Chemical Society*, **1966**, 88, 3888-3890.

[14] Minchinton AI, Tannock IF. *Nat Rev Cancer*. **2006** Aug; 6 (8): 583-92.

[15] Strauss, U. P.; Jackson, E. G. *Journal of Polymer Science* **1950**, 6, 649–659.

[16] Blockzijl W, Engberts JBFN. *Angew Chem Int Eng* **1993,** 32:1545.

[17] Nokaly MA. Polymer association structures, ACS Symposium Ser. 384, *Am Chem Soc*, **1989,** Washington DC.

[18] D. Cochin, F. Candau, et al. Direct imaging of microstructures formed in aqueous-solutions of polyamphiphiles. *Macromolecules*, 25, **1992**, pp. 4220–4223.

[19] Kegang Liu, Xiaohua Jiang and Patrick Hunziker. Carbohydrate-based amphiphilic nano delivery system for cancer therapy. *Nanoscale.* **2016.**

[20] Liechty, W.; Kryscio, D.; Slaughter, B.; Peppas, N. *Annu Rev Chem Biomol Eng.*

[21] E.S. Gil, S.M. Hudson. "Stimuli-responsive polymers and their bioconjugates." *Prog. Polym. Sci*., 29 (12). **2004**. 1173–1222.

[22] Moad, G.; E. Rizzardo; S. H. Thang. "Radical addition fragmentation chemistry in polymer synthesis". *Polymer*. **2008.** 49 (5): 1079–1131.

[23] Park, S. Y.; Bae, Y. H. *Macromol. Rapid Commun.* **1999**, *20* (5), 269–273.

[24] J. Kopeček and H. Bažilová, *Eur. Polym. J.*, **1973**, 9, 7–14.

[25] Parsons, et al. Block ionomer complexes consisting of siRNA and aRAFT-synthesized hydrophilic-*block*-cationic copolymers II: the influence of cationic block charge density on gene suppression. *Polym. Chem.*, **2016**. 7, 6044.

[26] Wan, Wen-Ming, et al. Structurally controlled "polysoaps" *via* RAFT copolymerization of AMPS and *n*-dodecyl acrylamide for environmental remediation. *Polym. Chem.*, **2014**. 5, 819.

[27] Kalyanasundaram, K. *Photochemistry in Microheterogeneous Systems*; Academic Press, Inc.: Orlando, FL, **1987**.

[28] Winnik, F. M. *Chem. Rev.* **1993**, *93* (2), 587–614.

Appendix

Synthesis of CEP

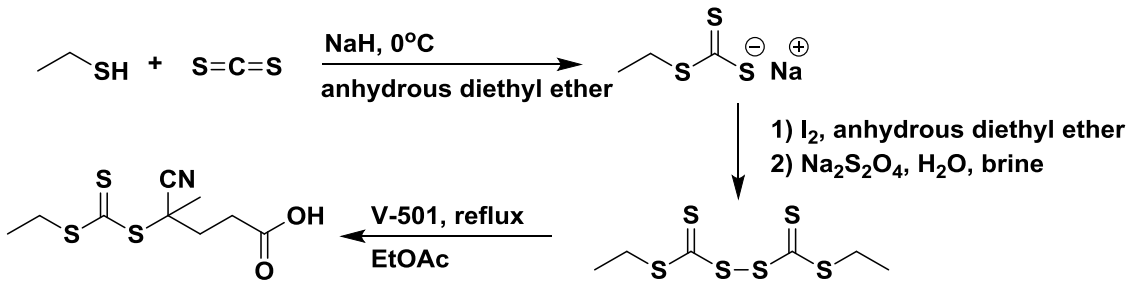

Scheme A1. Synthesis of RAFT chain transfer agent, CEP.

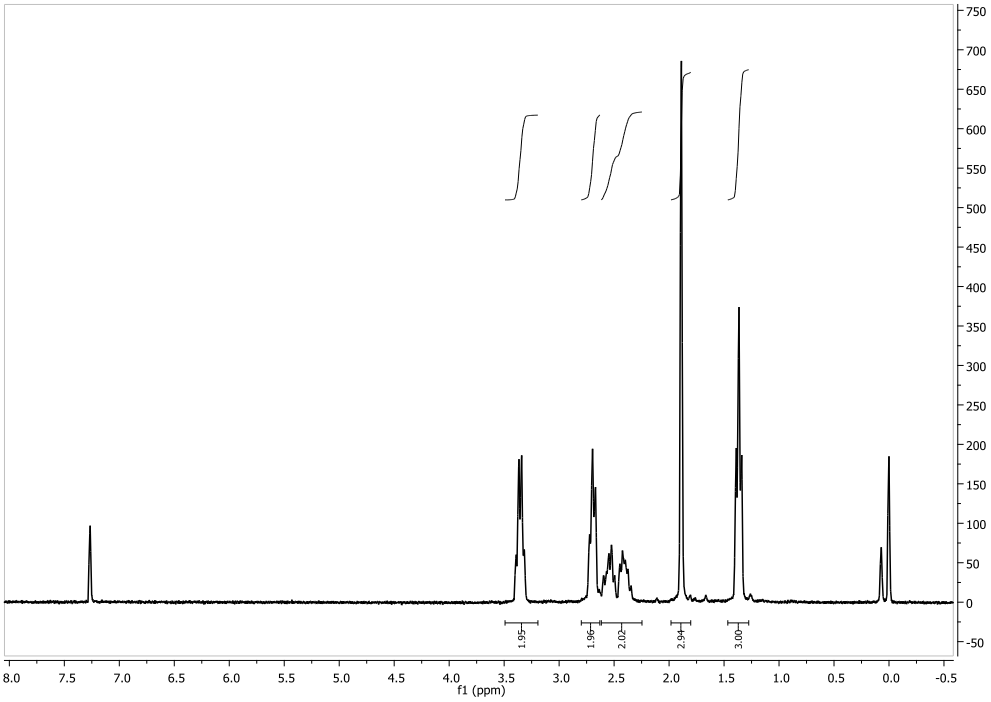

Figure A1. ^{1}H-NMR of CEP.

Synthesis of HPMA

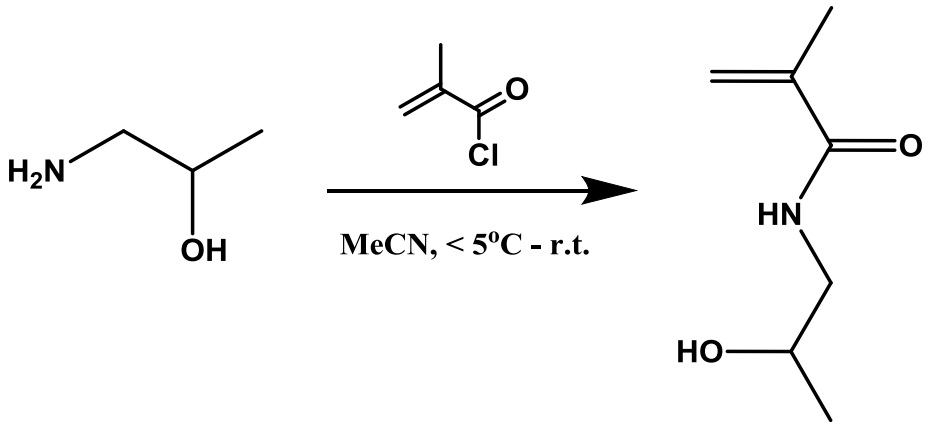

Scheme A2. Synthesis of HPMA.

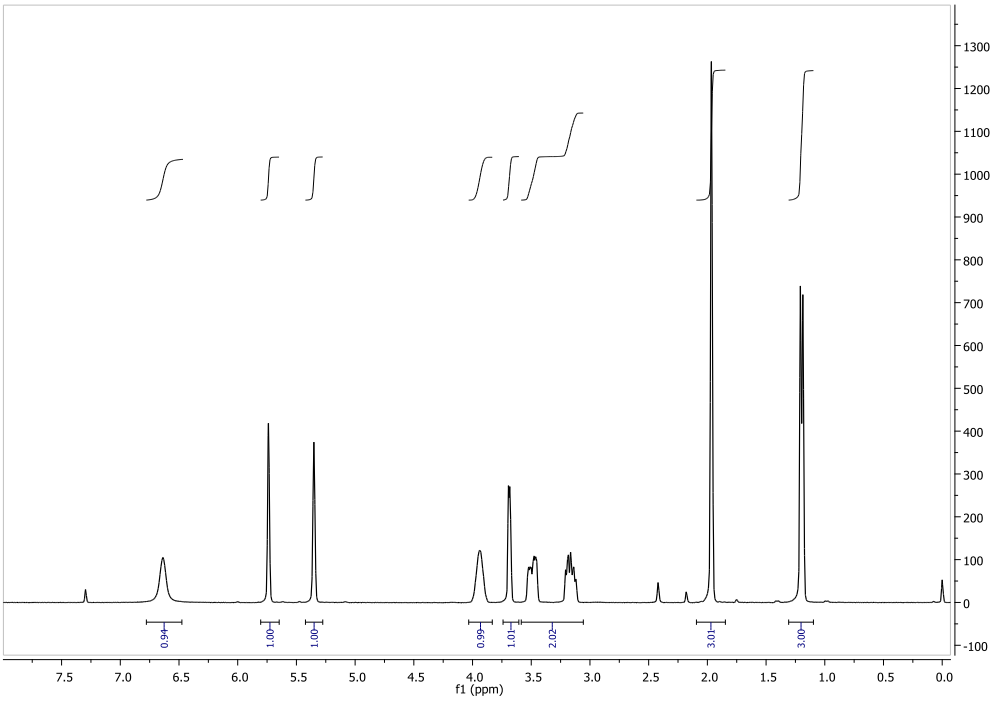

Figure A2. ^{1}H-NMR of HPMA.

Synthesis of DPDMA

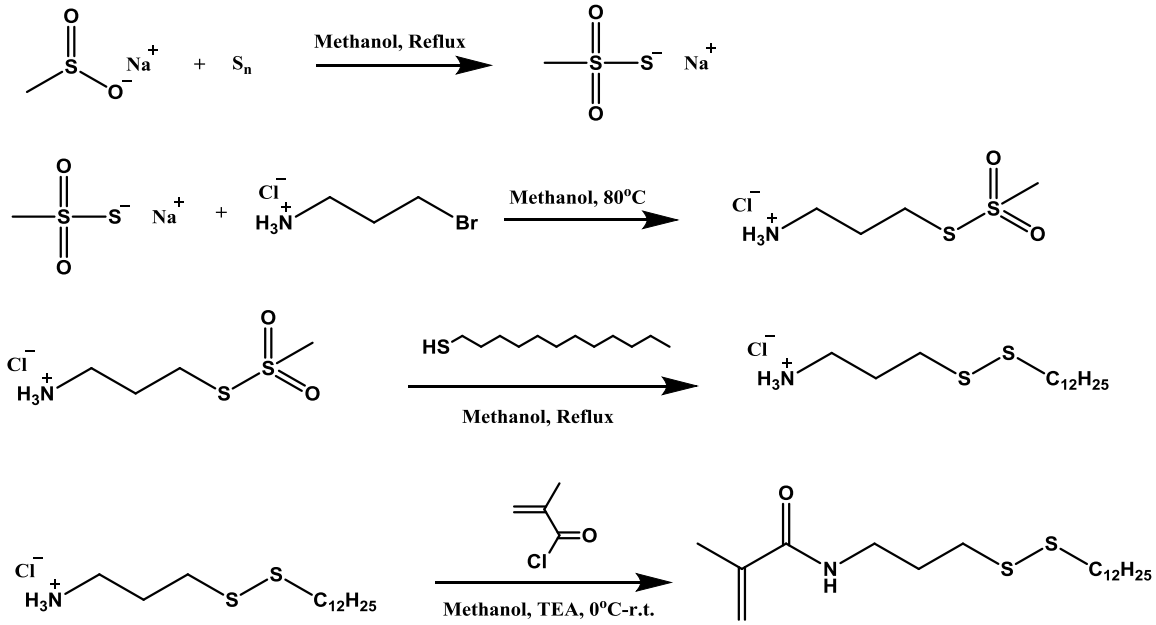

Scheme A3. Synthesis of DPDMA.

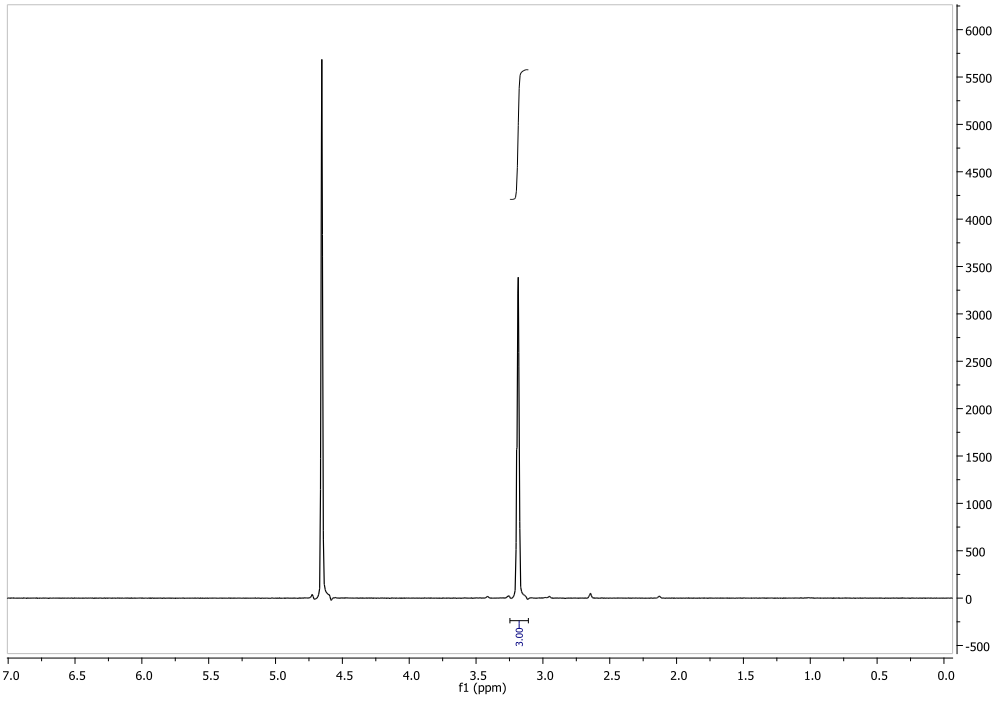

Figure A3. ^{1}H-NMR of sodium methanethiosulfonate.

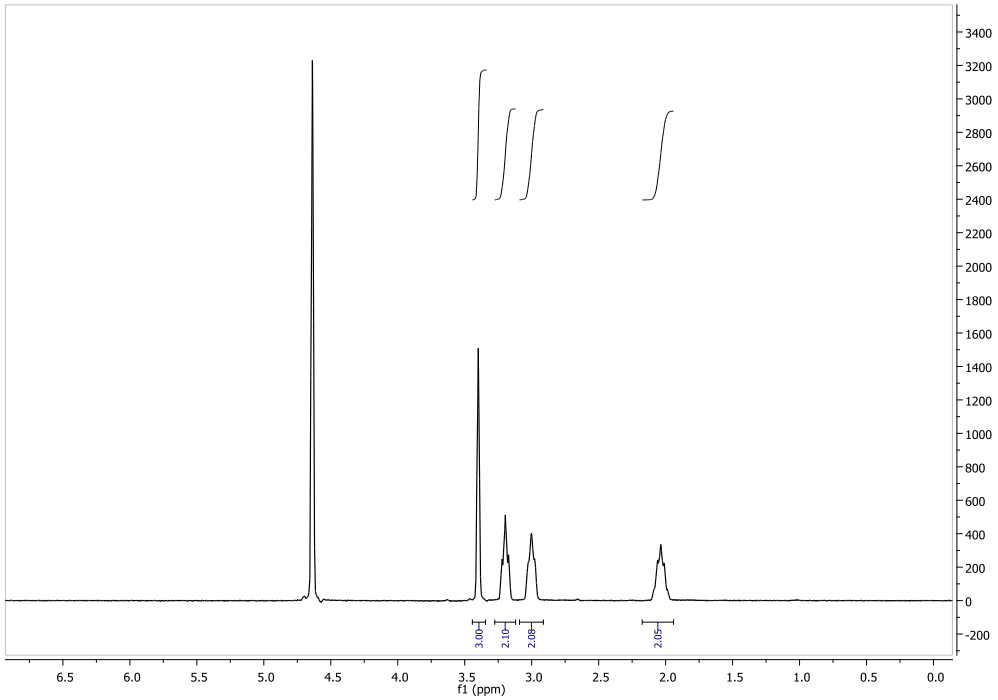

Figure A4. ^{1}H-NMR of aminopropyl sodium methanethiosulfonate.

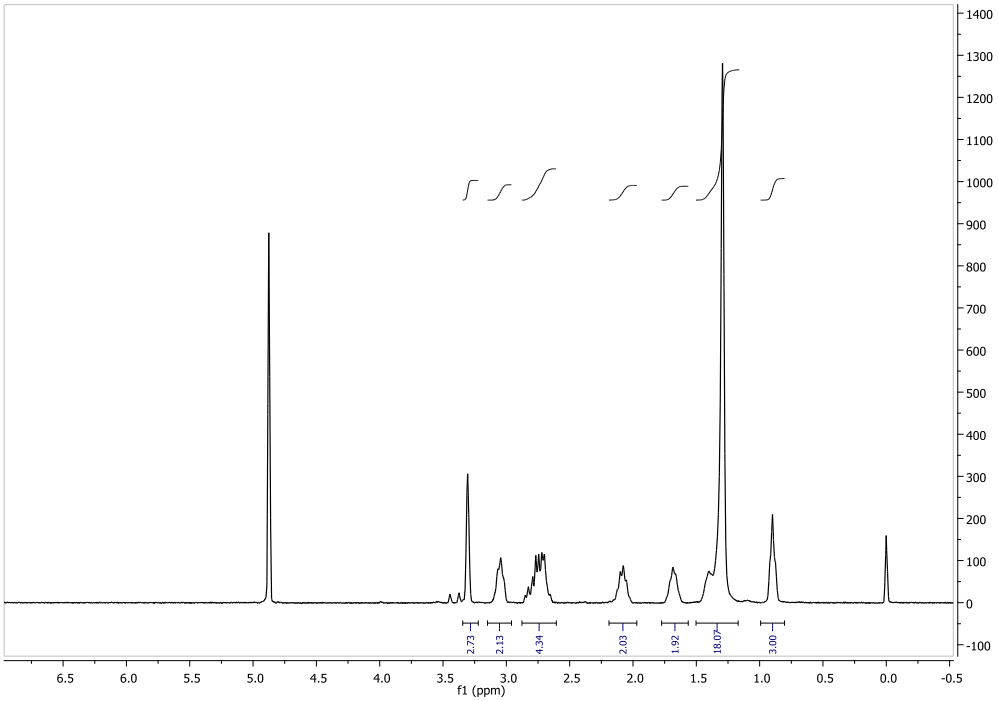

Figure A5. ^{1}H-NMR of aminopropyl dodecyl disulfide.

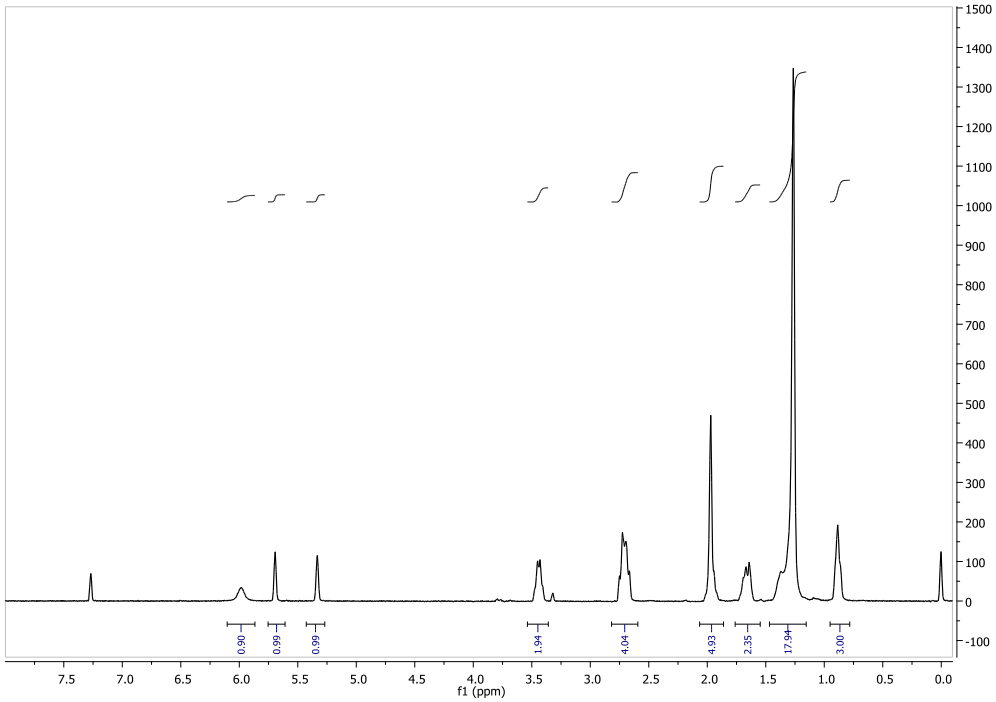

Figure A6. ^{1}H-NMR of DPDMA.

^{1}H-NMRs of polysoaps

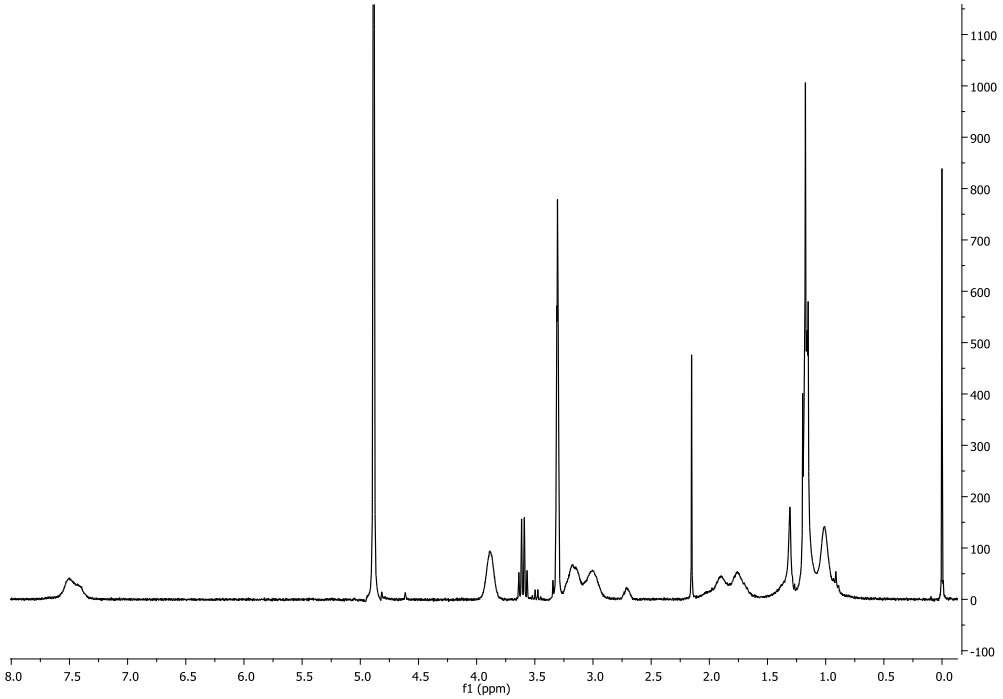

Figure A7. ^{1}H-NMR of 5% DPDMA polysoap.

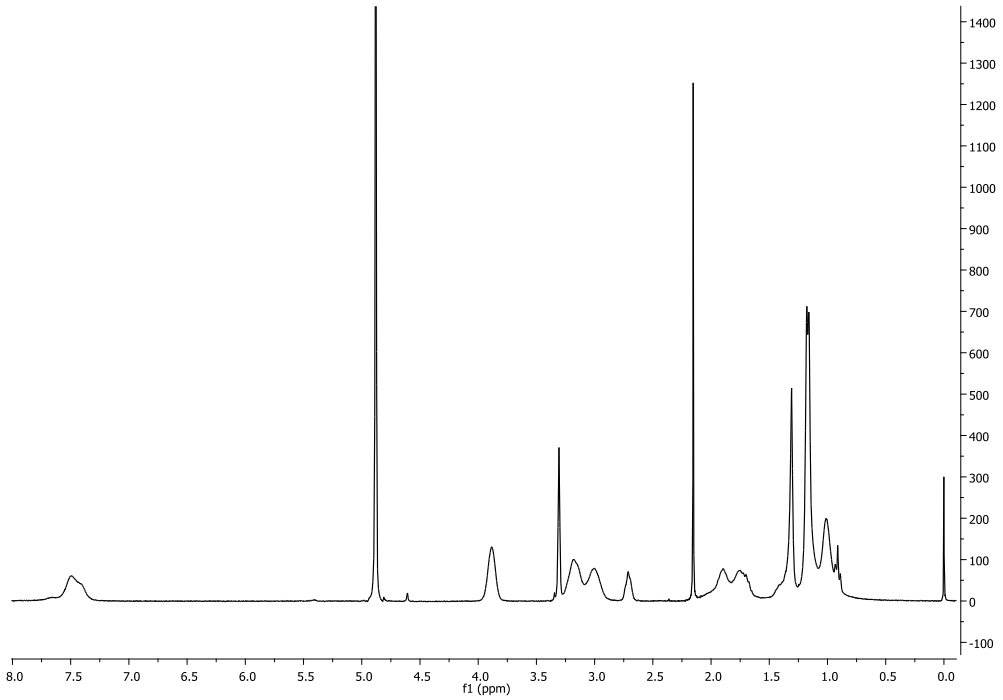

Figure A8. ^{1}H-NMR of 10% DPDMA polysoap.

Dynamic light scattering data processing

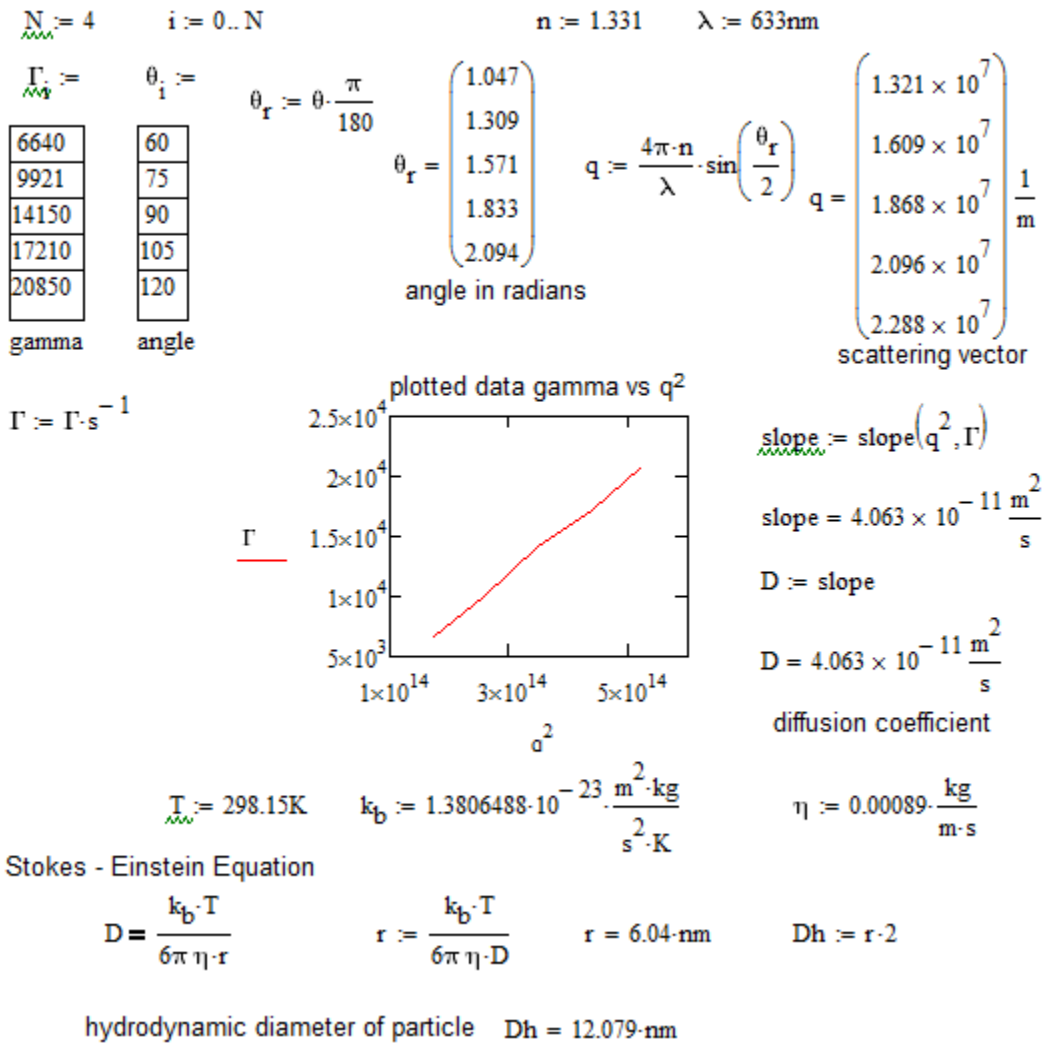

Figure A9. An example of DLS data processing using Mathcad of the 5% DPDMA sample at 5 mg/mL.

Dynamic and static light scattering data

Table A1. Calculated DLS and raw SLS data.

Concentration (mg/mL)	Dh (nm)	I (kcps)	std (of I)
	5% DPDMA		
5.0	12.0	83.3	0.94
3.0	11.6	56.4	1.12
1.9	12.6	37.1	0.80
1.0	11.3	22.1	1.33
0.5	14.9	12.0	0.43
0.1	11.3	4.33	0.18
	10% DPDMA		
5.0	56.1	919	14.6
3.0	57.5	693	11.3
2.0	59.4	539	8.44
1.0	58.4	348	6.30
0.5	59.9	198	3.85
0.1	60.6	34.8	0.63

*DLS data determined from autocorrelation functions at 60, 75, 90, 105, and 120^{o}.
*SLS data determined from raw scattering intensities at 90^{o}.